Journal of Advanced Research in Fluid Mechanics and Thermal Sciences

Journal homepage:
https://semarakilmu.com.my/journals/index.php/fluid_mechanics_thermal_sciences/index
ISSN: 2289-7879

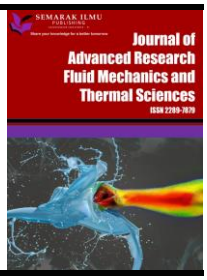

Numerical Investigation of Thermal Performance Enhancement of Solar Reservoir using Flash Cycle

Pritosh Tomar[1], Prateek Chauhan[2], Ashwani Kumar[3,*], Anoop Kumar Shukla[4], Víctor Daniel Jiménez Macedo[5], Bajarang Prasad Mishra[6], Nageswara Rao Lakkimsetty[7], Tadaga Channaveerappa Manjunath[8]

[1] Mechanical Engineering Department, Womens Institute of Technology, Veer Madho Singh Bhandari Uttarakhand Technical University Dehradun, India
[2] Department of Mechanical Engineering, Uttarakhand Technical University Dehradun Uttarakhand, India
[3] Technical Education Department, Uttar Pradesh Kanpur, 208024, India
[4] Department of Mechanical Engineering, Amity University Uttar Pradesh, Noida, India
[5] Mechanical Engineering Faculty, Michoacan University of Saint Nicholas of Hidalgo, Mexico
[6] Department of Electronics and Communication Engineering, JSS Academy of Technical Education Sector-62, Noida Uttar Pradesh, India
[7] Department of Chemical and Petroleum Engineering, School of Engineering & Computing, The American University of Ras Al Khaimah (AURAK), Ras al Khaimah, United Arab Emirates
[8] Department of Electronics and Communication Engineering, Dayananda Sagar College of Engineering, Bangalore Karnataka, India

ARTICLE INFO

Article history:
Received 26 May 2024
Received in revised form 6 October 2024
Accepted 15 October 2024
Available online 30 October 2024

Keywords:
Solar reservoir; solar radiation; heat transfer enhancement; clean energy; lower convection zone

ABSTRACT

The main objective of this research is to model a solar reservoir system located in Dehradun, Uttarakhand, India. Solar reservoir acts as both a collector and long-term storage for thermal energy, potentially providing heat for a full year. Using a single input, the latitude angle, solar radiation for the location is calculated. A one-dimensional time-dependent steady-state model is employed to predict the annual temperature behavior within the storage zone of the solar reservoir. The model analyses the temperature range achievable in the lower convection zone (LCZ) of the reservoir. The findings suggest that the LCZ can reach temperatures as high as 80°C. Additionally, the study demonstrates that an increase in feed temperature can improve overall system efficiency. At the end of summer, temperatures as high as 70 °C were observed in the solar pond at a depth of 1.32 m. It reached 26 °C at its lowest point in early April. In an artificial solar pond, salt water is utilised to inhibit convection. There was a 26% concentration of salt NACL at the lake's bottom. The kind and concentration of salt have an impact on the pond's stability. It was determined that 80 g/kg of water is the ideal salt level for the small solar pond. This study demonstrates the potential for maintaining both salinity gradient and thermal performance over an extended period. Future research efforts could benefit from larger-scale experiments that bridge the gap between controlled environments and real-world applications.

* *Corresponding author.*
E-mail address: drashwanikumardte@gmail.com

https://doi.org/10.37934/arfmts.123.1.197221

1. Introduction

The greatest renewable energy source is the sun, which is widely available around the planet. In actuality, it's among the finest substitutes for non-renewable energy sources. Since prehistoric times, humanity has used solar energy, radiant light and heat from the sun in very basic ways. Prior to 1970, a few nations conducted research and development to better utilize solar energy, but the majority of this effort remained only academic in nature. Following the significant increase in oil costs throughout the 1970s, several nations initiated comprehensive research and development initiatives to harness solar energy. From heating homes to generating electricity, various solar technologies hold immense potential in addressing pressing global challenges. These technologies, including solar heating, photovoltaic, thermal power, and architecture, can be broadly categorized as either passive or active based on their method of capturing and utilizing solar energy. Active systems, like photovoltaic panels and solar collectors, directly convert sunlight into usable forms. Abdelaziz and Saxena *et al.,* [1] and Vo *et al.,* [2] has investigated that solar thermal energy (STE) is an innovative method for capturing solar heat, is further classified by the US Energy Information Administration into low, medium, and high-temperature categories. While low-temperature collectors, typically flat plates, are used for applications like pool heating, medium-temperature ones (often flat plates as well) heat air or water for residential and commercial purposes. High-temperature collectors, however, leverage concentrated sunlight through mirrors or lenses to generate electricity. Unlike photovoltaic, which convert sunlight directly into electricity, STE focuses on capturing thermal energy [1,2].

Bacha *et al.,* [3] states that solar energy is a diluted energy source and the average daily solar energy incidence in India is only 5 Kwh/m^2 day. It requires extensive initial capital expenditure and must be gathered across a wide region. Additionally, solar energy is an intermittent energy source, thus, storage must be a part of a solar energy system in order to meet energy demands on overcast and evening hours. This causes the capital cost of these systems to rise even more. Using a sizable body of water, such as a solar reservoir, to absorb and store solar energy is the solution to this issue [4,5].

Solar ponds provide a unique platform for studying fundamental fluid dynamics phenomena and optimizing thermal energy systems [6]. Researchers can leverage the stratified layers and controlled environment of the pond to investigate topics like double diffusive convection, the complex interaction of wind and waves, and fluid flow behavior in stratified environments. Additionally, the availability of advanced equipment on-site facilitates cost analyses, comprehensive system studies, heat exchanger performance evaluations, and in-depth energy efficiency investigations [7,8].

2. Description of a Solar Reservoir

Solar reservoir novel approach to solar energy capture utilizes a saltwater pool as a large-scale solar collector, capable of storing thermal energy for later use. This system relies on a naturally occurring phenomenon called a halocline, where the pools saltwater separates into distinct layers of varying salinity [9-11]. Less salty water forms a layer on top, while saltier, and therefore denser, water settles at the bottom. This stratification traps heat from the sun in the lower depths, functioning as a built-in thermal reservoir [12,13]. With a depth of typically 3-4 meters, a durable plastic liner safeguards the bottom. This liner is a composite material, often constructed from woven polyester yarn (XB-5) for strength, high-density polyethylene (HDPE) for overall durability, and low-density polyethylene (LDPE) for flexibility. Additionally, hypalon, bonded with nylon mesh, enhances the liner's resistance to punctures and harsh weather conditions. The saltwater solution within the pool

varies in salinity, ranging from near 0% at the surface to a concentrated 20-30% at the bottom. This stratification is crucial for heat retention. However, if left undisturbed, natural diffusion will gradually weaken the salt concentration gradient over time. To keep the solar reservoir maintained, saline water runs out and fresh water is put at the top of the reservoir (due to evaporation losses, the amount of liquid added at top or bottom is larger than the amount withdrawn) [14,15]. Al-Jabri *et al.,* [9] states, concentration brine is introduced to the reservoir's bottom at the same moment. About 50–60 g of salt per square meter per day is needed for this purpose; this is a significant amount when seen annually. Because of this, it is customary to recycle the salt by using a nearby evaporation reservoir to evaporate the saline water runoff that rises to the surface. This process recovers the valuable salt for reuse, minimizing the need for external sources. To utilize the stored thermal energy, hot water is continuously drawn from the bottom of the reservoir and circulated through a heat exchanger. This process transfers heat to another system before the water is returned to the bottom. Alternatively, a heat exchanger coil can be immersed at the bottom to directly extract heat from the water. Figure 1 shows that the reservoir is divided into three distinct zones due to fluid movement and mixing patterns

i. Surface Convection Zone (SCZ): This top layer, typically 10-20 cm thick, has a nearly constant temperature close to the surrounding air. Salt concentration in this zone is low and uniform, almost zero.
ii. Non-Convection Zone (NCZ): This thicker zone, comprising over half the reservoir depth, exhibits increasing temperature and salinity with depth. It acts as an insulating layer, minimizing heat loss towards the surface. The NCZ also functions as a combined thermal storage and heat collection zone.
iii. Lower Convection Zone (LCZ): This bottom zone has similar thickness to the NCZ and features relatively constant temperature and salinity. The LCZ serves as the primary zone for both heat storage and collection, and is often referred to as the "storage zone" or "bottom layer."

Safi [6] investigated the solar pond and find that most of the incoming sunlight is absorbed by the bottom of the reservoir if the water is clear and has a high absorption rate. This absorption heats the water, causing it to expand and become less dense. In freshwater, this would trigger warm water to rise and cooler water to sink, creating convection current. However, due to the salinity gradient, a layer of denser saltwater forms at the bottom. This opposing density gradient prevents heat from rising through convection and escaping the reservoir. Consequently, while the surface temperature may stay around 30°C, the bottom can reach temperatures exceeding 90°C. The concentration of salt has an impact on the pond's stability [16,17]. A thorough explanation of the location of the heat extraction and the cross-sectional form of the tubes is given, since this modality is essential to the total efficiency. Then, in order to maximize performance and lower heat losses with the environment, several improving techniques have been presented in recent years, including floating rings, gels, porous materials, and phase change materials [18,19].

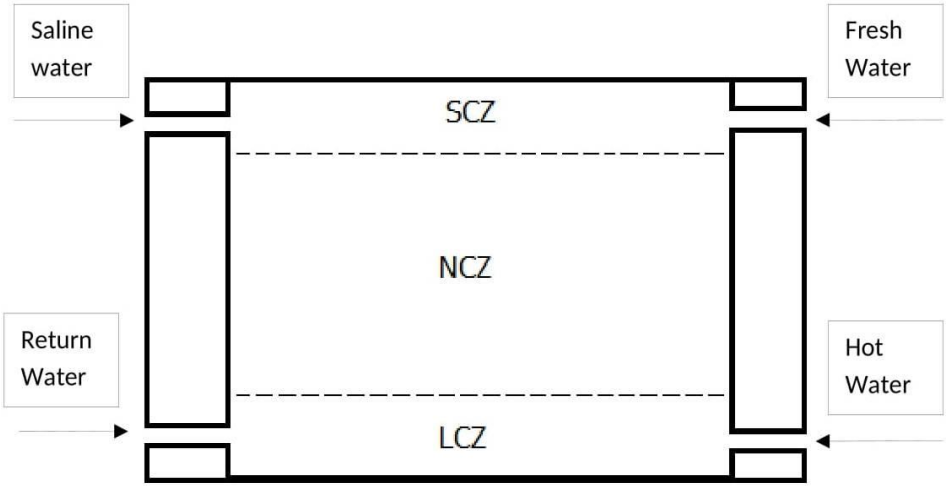

Fig. 1. Systematic illustration of a solar reservoir

As a result of the extraction of different raw resources, including as coal, non-ferrous metals, copper, and iron, brine water from the dewatering of deep mines is produced. After treating these fluids, extremely concentrated salt solutions are produced. These solutions can have powerful synergistic effects when paired with solar pond technology. The article offers a suggestion for the systemic use of the solar pond system together with preliminary, chosen simulation findings [20]. Solar Lake in Egypt serves as a natural example of this phenomenon in a salty body of water. The captured heat in the lower layer can be used to generate electricity through turbines like organic Rankine cycle turbines or Stirling engines. Alternatively, it can be utilized for heating buildings or industrial processes. Applications for this technology include process heating, desalination, refrigeration, drying, and even solar power generation [21,22].

2.1 Working Principle of Solar Reservoir

The solar reservoir utilizes a simple yet effective principle shown in Figure 2. As heat causes both air and water to expand and rise, like a hot air balloon. Similarly, sunlight heats regular reservoirs, causing the water to rise and release heat to the atmosphere, ultimately keeping the reservoir temperature near ambient [23,24]. The solar reservoir, however, cleverly prevents this heat loss by adding a layer of salt to the bottom. This dense layer, unlike the warmer and lighter water above, remains stationary due to its weight. The inspiration for this design came from naturally occurring saltwater lakes where the bottom layers exhibit significant temperature increases (around 40-50°C) [10]. These lakes naturally possess a salinity gradient, meaning the salt concentration increases with depth, keeping the denser, warmer water at the bottom. Imagine a reservoir with dissolved salt at a depth of L. This imaginary reservoir exhibits a gradual increase in salt concentration from the surface (C1) to the bottom (C2) [12].

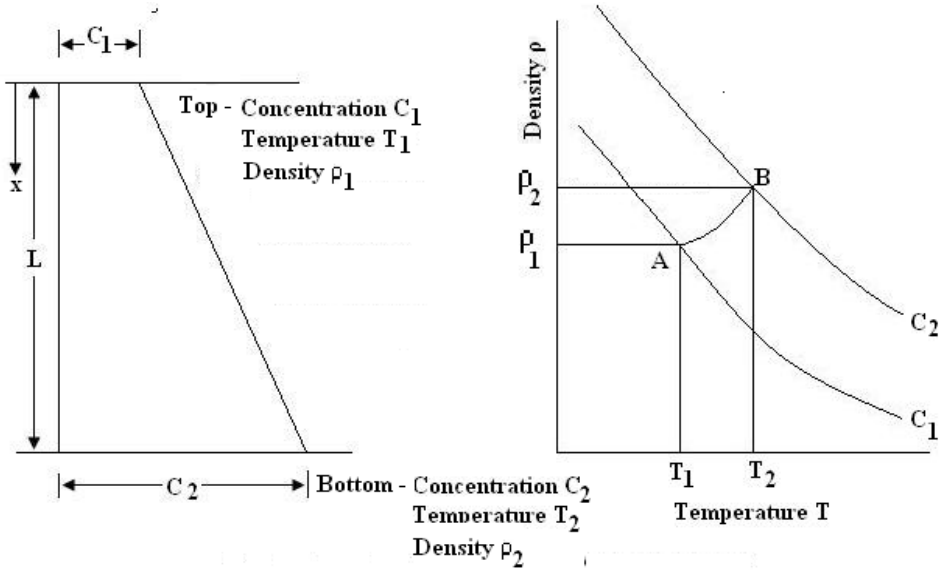

Fig. 2. Working principle of solar reservoir

Danso *et al.,* [14] studied the concept of solar reservoirs stems from the observation of certain natural lakes exhibiting significant temperature increases, reaching 40°C to 50°C in their deeper regions. This phenomenon occurs because these lakes naturally have higher salt concentrations at the bottom compared to the top, even during periods of intense heat. Imagine a reservoir with depth L, and consider the dissolved salts within the water [25]. Figure 2 shows a concentration gradient, where the concentration at the top (C1) is lower than the concentration at the bottom (C2). The Eq. (1) to Eq. (3) explores how the density of these two concentrations varies with temperature.

$$\frac{\partial \rho}{\partial x} > 0 \tag{1}$$

Considering that ρ = ρ(C, T), the stability requirement is

$$\left[\frac{\partial \rho}{\partial C}\right]_T \left[\frac{dC}{dx}\right] + \left[\frac{\partial \rho}{\partial T}\right]_C \left[\frac{dT}{dx}\right] > 0 \; or \; \frac{dC}{dx} > -\frac{\left\{\left(\frac{\partial \rho}{\partial T}\right)_C \left(\frac{dT}{dx}\right)\right\}}{\left(\frac{\partial \rho}{\partial C}\right)_T\}} \tag{2}$$

It may be demonstrated using a little more complex study that takes the impact of minor perturbations into accounts that

$$\frac{dC}{dx} > -\left\{\frac{\nu+\alpha}{\nu+D}\right\}\left\{\left(\frac{\partial \rho}{\partial T}\right)_C \left(\frac{dT}{dx}\right) / \left(\frac{\partial \rho}{\partial C}\right)_T\right\} \tag{3}$$

Where ν = kinematic viscosity.

D is the diffusivity of salt in water, and α is the thermal diffusivity. The ratio of (ν + α) to (ν + D) for a salt solution in water under solar reservoir conditions is around 1.15. As a result, compared to Eq. (2), the stability criteria provided by Eq. (3) is rather stricter. The minimal concentration gradient needed to keep a specific temperature gradient in a solar reservoir at a given level may be found using Eq. (2) or Eq. (3). In actual situation it is advised to allow for a certain margin of safety and to maintain the actual concentration gradient at a value that is about double that provided by Eq. (3).

2.2 Recent Technological Developments in Solar Reservoir

The early 20th century saw the discovery of a natural solar reservoir in Lake Medve, Transylvania, Hungary. By late summer, the lake's bottom reached a remarkable 70°C at a depth of 1.32 meters, contrasting with a cooler 26°C at its lowest point in early April. This phenomenon was attributed to the high salt concentration (26% NaCl) at the lake's bottom, which naturally inhibited convection currents. Inspired by this natural example, scientists developed artificial "salt gradient solar ponds," also known as solar reservoirs [15]. Research suggests an optimal salt concentration of around 80 grams per kilogram of water for these reservoirs.

A 2011 report by the International Energy Agency explored the potential for enhancing solar reservoir performance using a "multi-selective injection and withdrawal process." This advanced technique creates a temperature and salinity-sensitive layer within the reservoir, leading to a warmer layer near the bottom and reduced heat loss to the environment. The agency emphasizes the long-term benefits of solar energy technologies, highlighting their affordability, clean nature, limitless potential and applications in residential and commercial buildings [26-28]. These benefits include increased sustainability, reduced pollution, lower climate change mitigation costs, and a stabilizing effect on fossil fuel prices. Additionally, solar energy enhances a nation's energy security and reduces reliance on imported resources. The International Energy Agency acknowledges the initial investment costs associated with deploying this technology [29,30]. However, they view these costs as valuable "learning investments" that should be distributed strategically to maximize their impact.

Researchers have investigated transport processes within advanced solar ponds (ASPs) using simplified mathematical models. Their findings suggest that the multi-selective injection and withdrawal technique has the potential to significantly improve solar reservoir performance. In another study the fundamental principles of solar reservoirs were reviewed, along with the challenges encountered during their operation and maintenance. This aligns with our discussion on the factors influencing the technical and economic viability of solar reservoirs for both thermal applications and electricity generation [17].

Researchers have conducted experiments using a small model to understand temperature and salinity variations within the reservoir, in continuation the performance of a larger solar reservoir built in Turkey was analysed. Their findings suggest that the heat storage zone achieves the highest efficiency. However, a critical review of these studies reveals limitations. The small scale of the model in may not fully capture real-world conditions in larger reservoirs. Similarly, the specific performance values reported in the study by Verma *et al.,* [4] for a particular reservoir in Turkey might not be universally applicable to all solar ponds due to factors like size, location, and climate. Gasulla *et al.,* [31] investigated the effectiveness of various chemical treatments for controlling algae growth. Their findings suggest that cupricide is more effective than chlorine, particularly in improving water clarity within the upper and lower convection zones (LCZs) where light is crucial for algal growth. Valderrama *et al.,* [32] conducted a solar energy harvesting and storage experiment using a cylindrical concrete tank. Their approach involved adding hydrochloric acid (HCL) at different depths to regulate water clarity through acidification. The experiment achieved a stable salinity gradient within the reservoir by September 2009, which has been maintained to date. Following winter, the reservoir temperature steadily increased, reaching a peak of 55°C in August 2010. Additionally, studies investigating the economic feasibility and long-term maintenance requirements of solar reservoirs are crucial for their wider adoption [33].

3. Materials and Method

The first step in assessing the solar reservoir's effectiveness is figuring out how the radiation incident—or solar radiation geometry—is absorbed, transmitted, and reflected through the water.

3.1 Solar Radiation Geometry

The daily rotation of the globe, the yearly rotation of the tilted earth, and the latitude of the surface in issue all influence the angle at which the sun is visible from a given place on the surface. The earth's daily rotation is expressed by the solar hour angle, ω. The solar hour angle increases by 15° per hour as the planet revolves 360° in a 24-hour period. The solar hour angle is 0 at the sun's highest position in the sky. Angles count positively after noon, and negatively before. The solar azimuth angle, γ, which is the angle formed by the sun and due south, changes with the earth's rotation, going from -90° at dawn (east) to +90° at sunset (west). The angle formed by the surface with the horizontal is known as the slope angle, or β. The range is 0 to 1800 [21,22,26].

The sun's angular position with regard to the equator plane during solar noon is known as the declination angle, or δ. According to, it changes from -23.45° at the winter solstice to +23.45° at the summer solstice.

$$\delta = 23.45\, Sin\, \left[\frac{360}{365}(284 + n)\right] \tag{4}$$

As previously, the day in the year with n = 1–365 is indicated by n.

The latitude, ϕ, modifies the zenith angle further for sites other than the equator.

The zenith angle, θ, is a measure of an area's orientation relative to the sun and is inversely correlated with latitude, day, and time. The cosine of the zenith angle must be multiplied by the peak intensity in order to obtain the intensity.

$$Cos\, \theta = Sin\, \phi\, (Sin\, \delta\, Cos\, \beta + Cos\, \delta\, Cos\, \gamma\, Cos\, \omega\, Sin\, \beta) + Cos\, \phi\, (Cos\, \delta\, Cos\, \omega\, Cos\, \beta - Sin\, \delta\, Cos\, \gamma\, Sin\, \beta\,) + Cos\, \delta\, Sin\, \gamma\, Sin\, \omega\, Sin\, \beta \tag{5}$$

Special cases of above equation are normally required. Some of these are as follows,

Vertical surface β = 90^o,

$$Cos\, \theta = Sin\, \phi\, Cos\, \delta\, Cos\, \gamma\, Cos\, \omega - Cos\, \phi\, Sin\, \delta\, Cos\, \gamma + Cos\, \delta\, Sin\, \gamma\, Sin\, \omega \tag{6}$$

Horizontal surface β = 0^o,

$$Cos\, \theta = Sin\, \phi\, Sin\, \delta + Cos\, \phi\, Cos\, \delta\, Cos\, \omega \tag{7}$$

The complement of the zenith angle is also used quite often in calculations. It is called the solar altitude angle [34].

3.2 Reflection-Refraction-Based Transmissivity at the Air-Water Contact

A light beam of intensity Ibn passing through a transparent medium (air) is reflected and refracted when it reaches the interface dividing it from another transparent medium (water) (Figure 3). The reflected beam is oriented so that the angle of incidence and reflection are equal, and it has a lower intensity (Ir). Snell's Law, on the other hand, indicates that the incident and refracted beam directions are connected to one another [11-13].

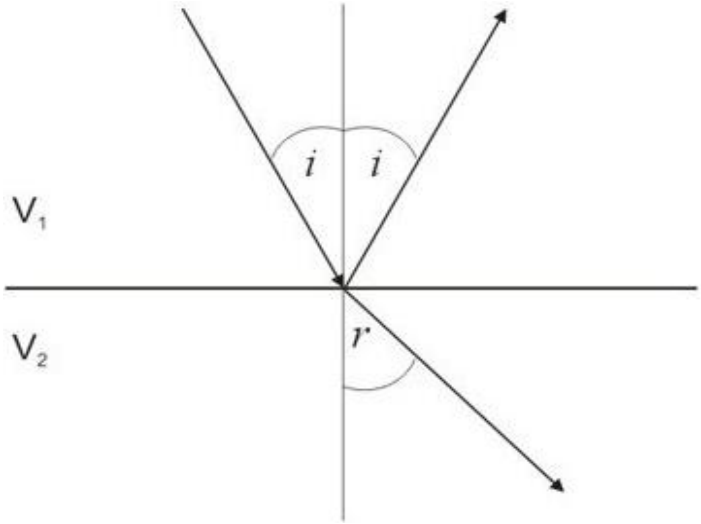

Fig. 3. Reflection and refraction at the air-water interface

$$\frac{Sin\ \theta_1}{Sin\ \theta_2} = \frac{n_1}{n_2} \tag{8}$$

When the angle of prevalence, θ1, is.
θ2 is a reflected angle, and
n_1, n_2 = refractive index of two media (air and water).

The refractivity is ρ

$$\rho = \frac{1}{2}(\rho_{\mathrm{I}} + \rho_{\mathrm{II}})(3.2.2)\rho_I = \frac{Sin^2(\theta_2-\theta_1)}{Sin^2(\theta_2+\theta_1)}(3.2.3)$$

$$\rho_{II} = \frac{tan^2(\theta_2-\theta_1)}{tan^2(\theta_2+\theta_1)} \tag{9}$$

So that, Tranmissivity (τ_r) based on the reflection and refraction at the air-water interface is

$$\tau_r = (1-\rho) \tag{10}$$

Sajid and Bicer [35] investigated that for the energy collection in the reservoir, one is generally not interested in large angles of incidences because these are associated with low values of radiation.

3.3 Transmissivity based on Absorption

By assuming that the attenuation caused by absorption is proportionate to the local intensity, one may determine the transmissivity based on absorption (Bouger's Law). Imagine an intense beam (Ibn) that is generally incident on a clear cover (δc) and emerges with an intensity (Il) (Figure 4).

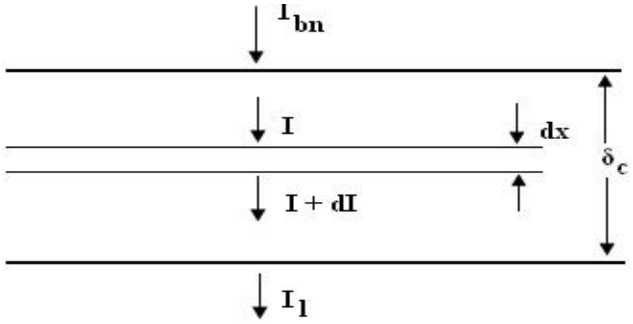

Fig. 4. Absorption in a transparent cover

From Bouger's Law

dI = -KI dx

where K, also known as the extinction coefficient, is a constant of proportionality. It will be taken for granted that its value is wavelength-independent. When the beam's length is integrated, we obtain

$$\tau_a = \frac{I_l}{I_{ba}} = e^{-K\delta_C} \tag{11}$$

If the beam is incident at an angle θ1, then (δC/Cos θ2) is the route that passes through the cover; θ2 is the angle of refraction. Next, Eq. (11) gets modification to the form

$$\tau_a = e^{-K\delta_C/\cos\theta_2} \tag{12}$$

But of water experimental data indicates that the extinction coefficient K is strong function of wavelength. Keeping this dependence in mind, Rebl and Nielsen have modified Eq. (11) into the following form which is the sum of four exponentials.

$$\tau_a = \sum_{j=1}^{4} A_j e^{-K_j x} \tag{13}$$

where x = water depth. Fitting the relevant experimental data yields the following values for the constants Aj and Kj.

The four values of A in Eq. (13) corresreservoir to the wavelength range 0.2 to 1.2 μm and add up to 0.776. Thus, only 77.6 per cent of the radiation is accounted for. The balance of 22.4 per cent corresreservoirs to radiation of wavelengths more than 1.2 μm, which is taken up by the body by very near to the surface within the first 1 or 2 cm. The above equation is valid for all depths excepting the first 1 or 2 cm.

An alternative and simple equation for calculating τ_a

$$\tau_a = 0.36 - 0.08 \ln x \tag{14}$$

where x = depth of water in meters. This equation has the same accuracy as Eq. (13) and is also valid for x > 0.01 m. In case of seldom radiation it is advised, for both Eq. (13) and Eq. (14) that x can be replaced by ($x/\text{Cos}\ \theta_2$), where θ2 is the refractive angle [36].

3.4 Daily-Average Total Extra-Terrestrial Radiation on a Horizontal Surface

Solar reservoir location is influenced by seasonal changes in the sun's path, altering its altitude, azimuth angle, and daily sunshine duration. Lei and Patterson [37] investigated that, this variation significantly impacts incident solar radiation and consequently affects solar collector performance. For climate representation in computations, monthly averaged data work best, because hourly and daily values fluctuate seasonally and are too brief for comprehensive climate assessments. Seasonal and yearly readings lack accuracy in climate computations. Hence, this study adopts averaged monthly measurements. Utilizing MATLAB, a multi-script program employing finite difference methods for ordinary differential equations in steady-state models has been developed. The program accommodates changes surrounding circumstances and boundary conditions throughout time.

Calculating solar radiation for use in solar energy applications requires only the user's latitude as input. This information allows the software to predict sunrise, sunset, and sunshine duration. To determine the amount of solar radiation received at a specific location, several approaches are available. One option utilizes a recently developed and tested empirical equation, which has shown improved accuracy in locations like Jerusalem, Riyadh, and Kuwait. Additionally, references or NASA's 22-year average data can be used as a starting point, providing monthly average daily solar radiation values. It's important to note that the Earth's distance from the sun varies throughout the year, leading to changes in the apparent extraterrestrial solar irradiation. This seasonal variation, coupled with the number of daylight hours, directly influences the intensity of solar radiation received at any given location. The alien solar irradiation on a daily average is provided by

$$I_O = I_{SC}\left[1 + 0.003\cos\left(\frac{360N}{370}\right)\right] \tag{15}$$

Since the early 20th century, researchers, led by At the Smithsonian Institute, Abbott and his staff, conducted numerous studies to determine the solar constant (Isc). They proposed a value of 1353 W/m^2 after extensive research. Subsequent ground-based and high-altitude measurements upheld this value, leading to its acceptance as the standard solar constant. NASA, following space-based measurements, also recommended the value of 1368 W/m^2 as the generally accepted solar constant, recently published on NASA's website. This satellite-measured yearly average closely aligns with the std. value.

On a horizontal surface, the total daily extra-terrestrial radiation may be calculated using

$$H_{OT} = \frac{I_{OD}}{\pi}\left[\cos\theta\cos\delta\sin\omega + \frac{2\pi\omega}{360}\sin\varphi\sin\delta\right] \tag{16}$$

where I_{od} is the amount of daily total direct normal extraterrestrial radiation. It is calculated by taking the value of solar irradiation throughout the day as the extraterrestrial radiation.

$$I_{OD} = 24I_O \tag{17}$$

3.5 Concentration Profile in the Gradient Zone

Predicting the rate of salt diffusion from the lower to the upper CZ requires an understanding of the gradient zone's concentration profile form. The concentration profile is assumed to be linear by most researchers. This presumption is frequently broken. However, description of the gradient profile of salt concentration in a solar reservoir also takes into account the sloping walls [38].

Temperature has a significant influence on the salt's diffusion coefficient in water. The following temperature fluctuation of the diffusion coefficient has been proposed by Tabor and Weinberger.

$$D = 1.39\ (1 + 0.029\ (T - 20))\ *10^{-9} \tag{18}$$

T is in C, while D is in m^2/s.

The surface area of tiny solar reservoirs varies significantly with depth. Therefore, the one-dimensional steady state equation for salt diffusion has to be expressed as

$$\frac{\partial}{\partial Z}\left(AD\frac{\partial S}{\partial Z}\right) = 0 \tag{19}$$

where Z is the distance from the reservoir's surface, A is the area at depth Z, and S is the salt concentration in kg/m^3.

Unless there are abrupt variations in the salinity and temperature of the upper and lower mixed zones, the steady state assumption makes sense. The area of the reservoir at depth Z may be expressed as follows for a small solar reservoir with total depth "H," length L, width b, and side slope α.

$$A(Z) = [L + 2(H - Z)Cot\ \alpha][b + 2(H - Z)Cot\ \alpha] \tag{20}$$

Ab = Reservoir's bottom area = L * b.

For the purposes of calculating the diffusion coefficient, it is possible to assume that the temperature profile in the gradient zone of the solar reservoir is linear.

$$T = T_S + \frac{(T_b - T_S)(Z - Z_1)}{Z_2 - Z_1} \tag{21}$$

where,
TS = Temperature of the upper Convective layer of the reservoir,
Tb = Temperature of the lower convective layer of the reservoir,
Z1 = Interface between upper layer and gradient zone,
Z2 = Interface between LCZ and gradient zone.

One may integrate Eq. (19) once to obtain

$$AD\frac{\partial S}{\partial Z} = G, \tag{22}$$

where G represents the Kg/s constant salt diffusion rate.

You may integrate the aforementioned equations one more to get

$$S(Z_2) - S(Z_1) = G \int_{Z_1}^{Z_2} \frac{dZ}{AD}, \tag{23}$$

Where S (Z1) and S (Z2), which are typically known, are the salinities in the upper and LCZs. For a given salinity in the upper and lower convective layers, we may calculate the salt diffusion rate G using Eq. (18), Eq. (20), and Eq. (21) in Eq. (23). We can determine the salinity profile as soon as we know the salt diffusion rate.

$$\left(S(Z) - S(Z_1)\right) = \int_{Z_1}^{Z} \frac{G}{AD} dZ, \tag{24}$$

3.6 Temperature Distribution and Efficiency

Calculating the T flow in a solar reservoir, comprising three zones, is intricate. An exact solution involves solving specific differential equations for each zone, considering matching conditions at interfaces, and satisfying boundary conditions at the reservoir's surfaces. To streamline the complexity, a common practice is simplification. One prevalent formulation assumes the surface and LCZs as perfectly mixed layers with uniform temperatures changing only with time. This simplification is particularly effective when the reservoir's lateral dimensions significantly surpass its depth (L), ensuring predominant vertical temperature variation and constant properties. The resulting heat conduction equation is the source of the non-CZ differential equation [39].

$$\rho C_p \frac{\partial T_{II}}{\partial t} = k \frac{\partial^2 T_{II}}{\partial x^2} - \frac{dI}{dx} \tag{25}$$

With $I = I_b\tau_{rb}\tau_{ab} + I_d\tau_{rd}\tau_{ad}$.

The differential equations to be satisfied for the upper and lower layers of the reservoir are obtained by taking energy balance (Figure 5).

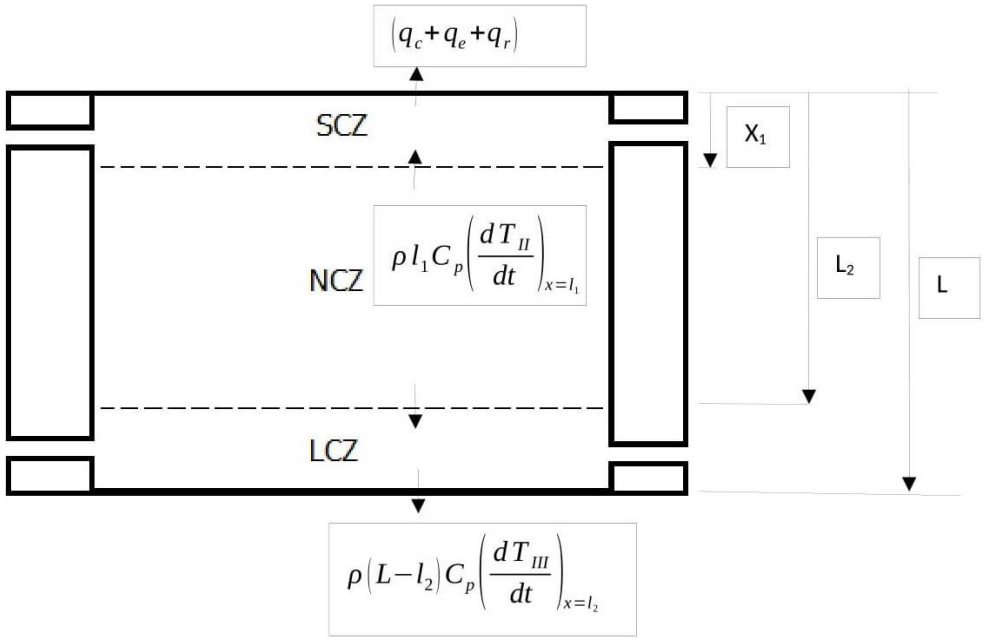

Fig. 5. Energy flows in and out of the surface and the LCZ

For the Surface CZ

Rate of change of energy contained in the surface CZ of thickness l_1 equal to the

(Rate of solar radiation absorbed in the layer l1) + (Rate of heat transfer from the non-CZ) - (Rate of heat loss from the upper surface due to convection, evaporation, and radiation).

$$\rho l_1 C_p \left(\frac{dT_{II}}{dt}\right)_{x=l_1} = k\left(\frac{\partial T_{II}}{\partial x}\right)_{x=l_1} + \left[(I)_{x=0} - (I)_{x=l_1}\right] - \frac{1}{A_p}(q_c + q_e + q_r) \tag{26}$$

For the LCZ

The rate at which heat is transmitted in from the non-CZ plus the solar radiation absorbed in the thickness l2 determine the rate of change of energy contained in the LCZ of thickness (L-l2). (The speed at which heat escapes to the earth below) (Usable Heat Extraction Rate).

Thus,

$$\rho(L - l_2) C_p \left(\frac{dT_{III}}{dt}\right)_{x=l_2} = -k\left(\frac{\partial T_{II}}{\partial x}\right)_{x=l_2} + (I)_{x=l_2} — k_g \left(\frac{\partial T_g}{\partial x}\right)_{x=L} - \frac{q_{load}}{A_p} \tag{27}$$

Solutions to the set of Eq. (25) to Eq. (27) have been obtained by many investigators. They have been solved for the situation when there is no useful heat extracted from the reservoir (q_{load}= 0), as well as when there is a heat extraction.

The first analytical solution for the differential Eq. (25) was provided using a superposition technique, considering radiation absorption separately at the surface, in the water body, and at the bottom. The problem was simplified by neglecting CZ thicknesses and assuming the reservoir surface temperature equals ambient air temperature. Weinberger used sine-cosine series for solar radiation on the reservoir and sine series for ambient temperature variation, estimating the temperature rise in a solar reservoir. Post-initial heating, energy extraction stabilizes, and Weinberger found a specific reservoir depth where the heat extraction rate is maximized, equalling solar radiation reaching the reservoir bottom [40].

Analytical study provided a way to address the yearly temperature fluctuations in a solar reservoir intended for room heating. A reservoir several meters deep with a surface CZ of insignificant thickness and a LCZ of limited thickness has been taken into consideration. When daily fluctuations are taken into account, the LCZ's temperature is calculated as follows

$$T_{III} = T_{III}^{*} + T_{III}^{**} Cos\ (\omega t - \delta)$$

where T_{III}* = annual average tem.in the LCZ, T_{III}** = amplitude, ω = frequency, and δ = phase lag behind changes in insolation. The heat conduction equation (3.6.1) in the steady state may be solved with ease to get the yearly average temperature TIII*, which is independent of time. We arrive to the following solution

$$T_{III}^{*} - T_a^{*} = \frac{\tau_r H_g^{*}}{k} \sum_{j=1}^{4} \frac{A_j}{K_j'} \left(1 - e^{-K_j' l_2}\right) - \frac{l_2}{k} \frac{q_{load}^{*}}{A_p} \tag{28}$$

The formula for calculating Kj' is (Kj / Cos θ2), where θ2 is the angle of refraction that corresreservoirs to an effective angle of incidence. Ta* is the yearly average ambient temperature, Hg* is the annual average global radiation.

The non-CZ bottom depth is represented by l2, and the yearly average heat extraction rate is represented by qload*.

A straightforward and practical formula for figuring out average performance or evaluating a solar reservoir's size for a particular need is Eq. (28).

Additionally, authors have examined the solar reservoir as a steady state apparatus and came up with a time-independent solution in terms of the yearly average values. Eq. (25) for the non-CZ decreases to in a steady state scenario.

$$k\frac{d^2T_{II}{}^*}{dx^2} = \frac{d}{dx}\left(H_g{}^*\tau_r\tau_a\right) = H_g{}^*\tau_r\frac{d\tau_a}{dx} \tag{29}$$

where the values of τ_r and τ_a are captured at the optimum contact angle. Combining once, we get

$$kT_{II}{}^* = H_g{}^*\tau_r\int_{l_1}^{x}\tau_a dx + c_1x + c_2 \tag{30}$$

where the integration constants c1 and c2 are
Changing the prerequisites,
TII* = TI* (a constant) at x = l1.

The formulas on the pattern of temperatures and variations in temperatures in the non-CZ may be found at x = l2, where TII* = TIII* (a constant) and c1 and c2 can be solved for. By using these formulae and realizing that, in a steady state scenario, the yearly average heat extraction rate from the reservoir is equal to the speed at that energy enters the system at the contact x = l2 LCZ, we obtain

$$q_{load}{}^* = A_p\left[\left\{\frac{H_g{}^*\tau_r}{(l_2-l_1)}\int_{l_1}^{l_2}\tau_a dx\right\} - \frac{k}{(l_2-l_1)}\{T_{III}{}^* - T_I{}^*\}\right] \tag{31}$$

The calculation of the solar reservoir's yearly average efficiency involves dividing both sides of the preceding equation by Hg*Ap. We obtain,

$$\eta^* = \left\{\frac{\tau_r}{(l_2-l_1)}\int_{l_1}^{l_2}\tau_a dx\right\} - \frac{k}{(l_2-l_1)}\left\{\frac{T_{III}{}^* - T_I{}^*}{H_g{}^*}\right\} \tag{32}$$

Using Rabl an Nielsen's Eq. (13) for τ_a and substituting K_j' for K_j, we get

$$\int_{l_1}^{l_2}\tau_a dx = \sum_{j=1}^{4}\frac{A_j}{K_j'}\left(e^{-K_j'l_1} - e^{-K_j'l_2}\right) \tag{33}$$

Thus, equations become

$$q_{load}{}^* = A_p\left[\left\{\frac{H_g{}^*\tau_r}{(l_2-l_1)}\sum_{j=1}^{4}\frac{A_j}{K_j'}\left(e^{-K_j'l_1} - e^{-K_j'l_2}\right)\right\} - \frac{k}{(l_2-l_1)}\{T_{III}{}^* - T_I{}^*\}\right], \tag{34}$$

$$\eta^* = \left\{\frac{\tau_r}{(l_2-l_1)}\sum_{j=1}^{4}\frac{A_j}{K_j'}\left(e^{-K_j'l_1}-e^{-K_j'l_2}\right)\right\} - \frac{k}{(l_2-l_1)}\left\{\frac{T_{III}{}^*-T_I{}^*}{H_g{}^*}\right\} \quad (35)$$

These formulas can be used to determine a solar reservoir's average performance or to estimate the size of a reservoir needed to meet a specific need.

3.7 Power Production in Dehradun Using a Solar Reservoir

One of the most dependable and cost-effective solar systems is the solar reservoir. Since the solar energy is collected and stored in a single system, the heat generated in the summer may be used in the winter. The mathematical formulas for calculating the parameters influencing the solar reservoir's performance are presented in the section 3.1-3.6 above in order to anticipate the potential of the solar reservoir at any location.

Based on location latitude, the daily monthly average techniques are used in the calculation of the sun's radiation intake to the reservoir. The impacts of any parameter depend how well the solar reservoir are predicted making intermittent and 1-D stable state assumptions in the gradient region [41].

This research proposes establishing a solar reservoir to contribute to Dehradun's (State Uttarakhand, Country India) power generation. To optimize the design MATLAB has been used. However, accurately predicting local temperatures remains a challenge. Therefore, historical temperature and relative humidity data from Dehradun for the past year has been used (Table 1, Figure 6).

Relative humidity plays a role alongside extraterrestrial radiation in affecting the overall performance of the solar reservoir. For electricity generation, the chosen working fluid is the reservoir brine itself. Flash distillation, a well-established, simple, and reliable technology, was selected for brine production.

Table 1
Environmental data for Dehradun

Month	Avg. Low Temperature °C	Avg. High Temperature °C	Ex. High Temperature °C	Rel. Humidity %	S.R. MJ/m^2/day
January	3	13	27	86	8.70
February	6	17	30	82	12.52
March	7	21	33	75	18.11
April	10	24	38	63	23.79
May	13	28	41	52	28.49
June	17	33	45	46	31.22
July	21	37	46	44	30.48
August	20	35	44	50	27.50
September	17	33	44	56	22.62
October	12	27	39	63	16.56
November	7	19	32	77	10.70
December	3	13	28	86	7.69

3.8 Flash Cycle

Figure 6 and Table 2 shows the flash cycle. The flash cycle was selected for the power plant system even though it was predicted to be the least efficient due to the flashing process's inevitable losses. In a flash cycle, heated reservoir brine is throttled to create low pressure steam. Steam and concentrated brine are produced when the brine flashes. The concentrated brine and steam are

separated in a flash separator. The pressure of saturation that matches the intended saltwater back heat is the separator pressure. Droplet size is decreased with a demister. A turbine expands the steam to condensing pressure. Condensed steam is released and brought back to the surface of the reservoir. Pumping is not necessary to achieve this return flow if the condenser is positioned enough above the surface. The salt water percentage in the reservoir is preserved and clean water is returned to the surface.

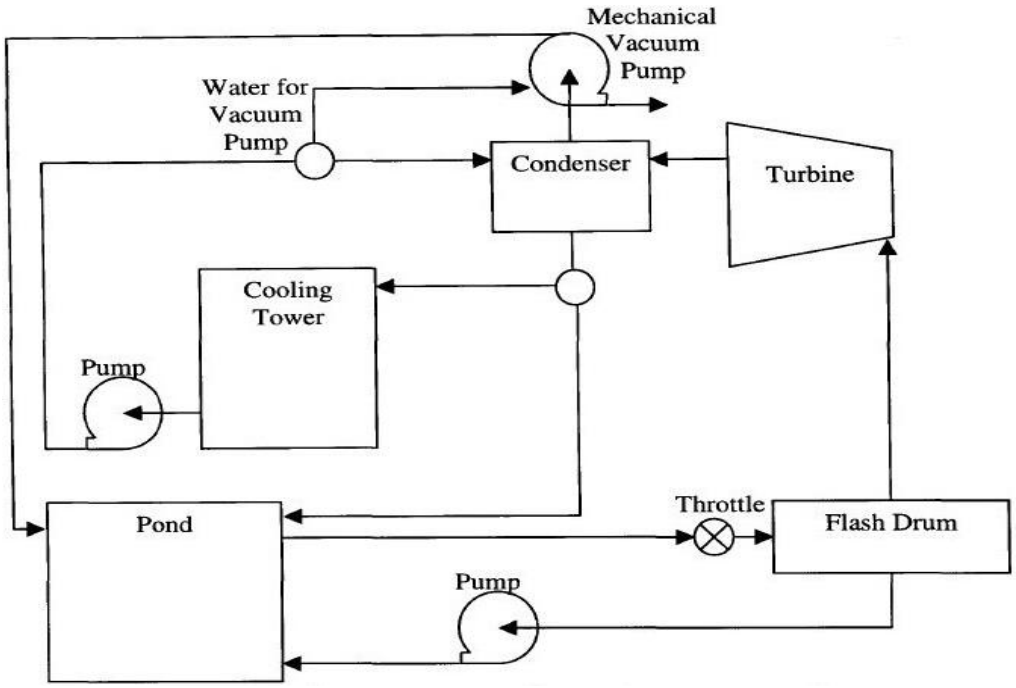

Fig. 6. Flash cycle for solar reservoir power generation in a salt gradient.

Table 2
Calculation for flash fraction

1	Estimate the flash fraction, f	$f = \frac{\dot{m}_w^v}{\dot{m}_{mix}^F}$
2	Calculate the salinity of the exiting liquid, S^L, as a function of the salinity of the feed, S^F, and the flash fraction, f	$S^L = \frac{S^F}{1-f}$
3	Calculate the enthalpy of the exiting liquid, h^L_{mix} from the correlations	$h_{mix}^L = h_{mix}^L(T_{Flash}, S^L)$
4	Calculate the enthalpy of the exiting liquid, h^F_{mix} from the correlations	$h_{mix}^F = h_{mix}^F(T_{Pond}, S^F)$
5	Calculate the enthalpy of the exiting liquid, h^v_w from the correlations	$h_w^v = h_w^v(T_{Flash}, P_{Flash})$
6	Recalculate the flash fraction from the 1st Law Analysis	$f = \frac{h_{mix}^F - h_{mix}^L}{h_w^v - h_{mix}^L}$
7	If the new flash fraction is sufficiently close to the old flash fraction, then quit; else let f = fnew and continue from step 2	

4. Results and Discussion

In Dehradun, India, the solar radiation is calculated using a single input latitude angle. The result is based on the solution provided in previous studies and the findings are displayed in Figure 7 for the sun radiation in Dehradun [19,42,43].

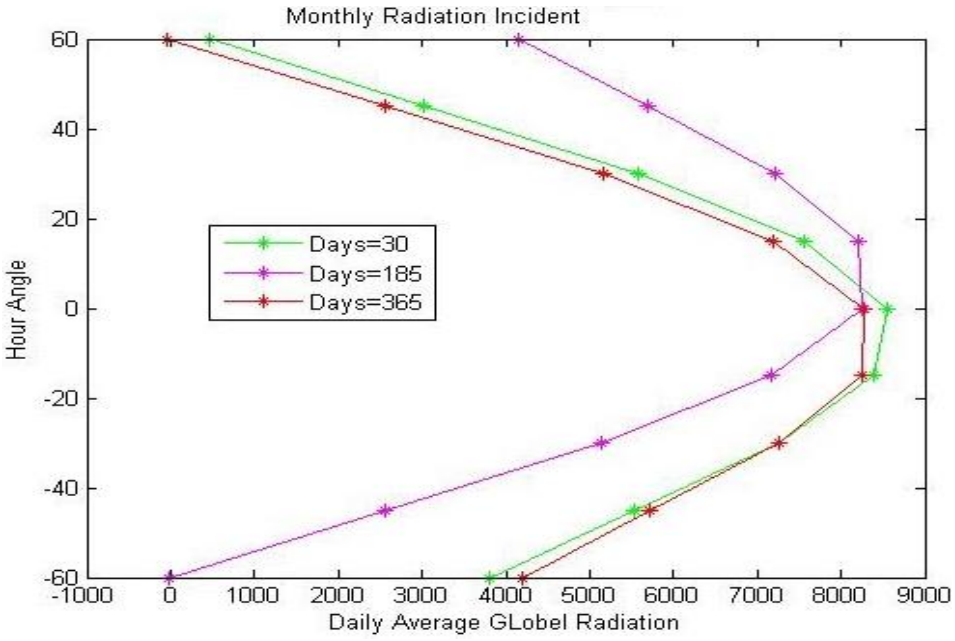

Fig. 7. The solar radiation incidence over Dehradun

Real-world temperature data collected by Rabl and Knooi over a year was used to develop a one-dimensional, time-varying steady-state equation that accurately predicts the solar pool's temperature pattern in the storage zone. This excellent agreement between the predicted and actual temperatures is shown in Figure 8.

The results presented in Figure 7 to Figure 10 are based on the calculations performed for the solar reservoir, as detailed in Section 3. All calculations were conducted using MATLAB. A single-input approach was employed to determine the temperature range achievable in the lower convection zone (LCZ) by the end of the year, starting from the reservoir's production date.

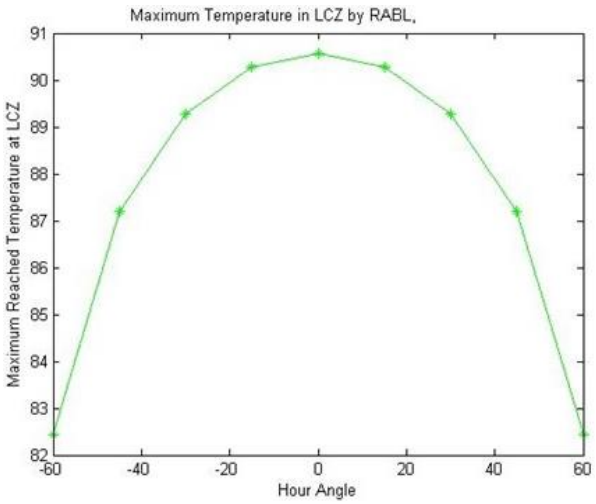

Fig. 8. The highest temperature attained all year long

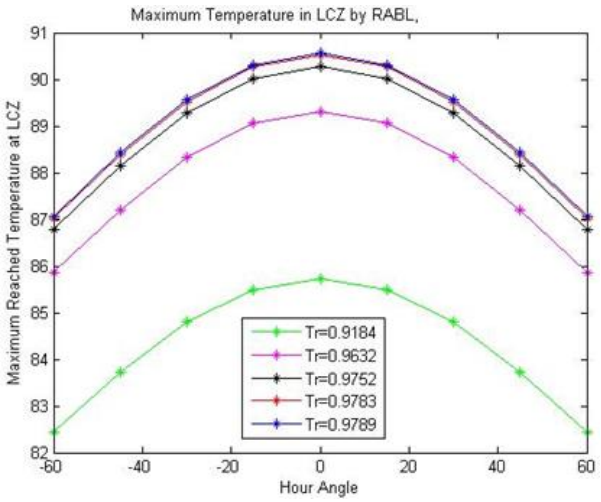

Fig. 9. Maximum temperature attained by Rabl during the course of the year

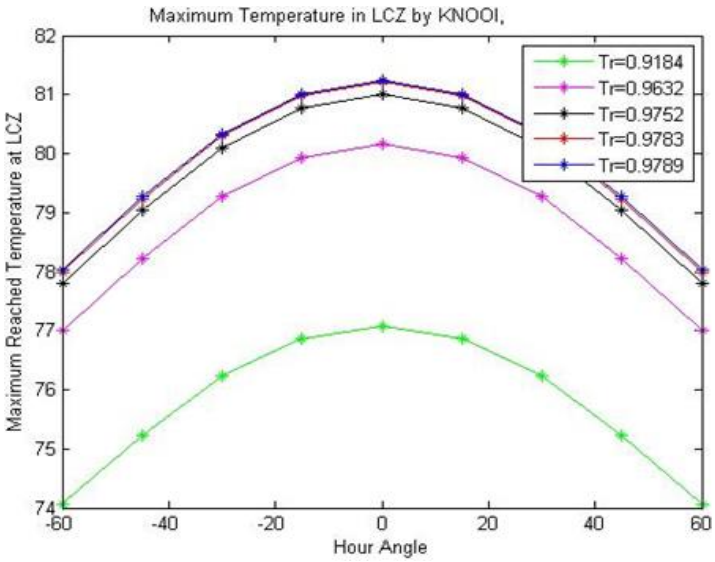

Fig. 10. Maximum temperature recorded by the Knooi solution annually

Figure 11 illustrates the relationship between varying flash pressures and their impact on both cycle efficiency and electricity generation. While reducing the flash pressure results in a smaller overall reservoir size, it concurrently leads to a positive outcome – an increase in cycle efficiency and 5 MW of electricity production.

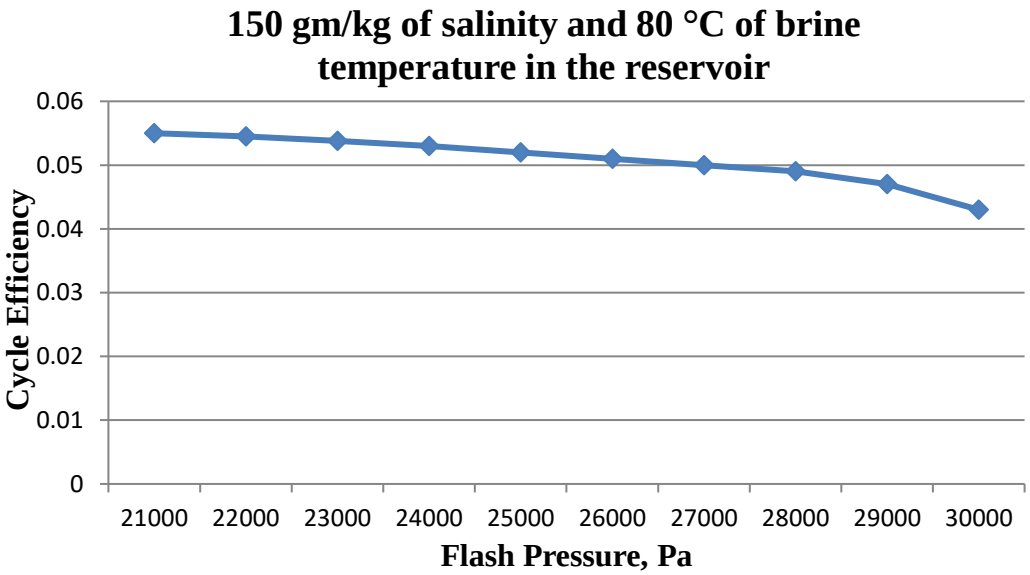

Fig. 11. Changes in flash pressure in relation to cycle efficiency

Figure 12 highlights the impact of varying flash pressure on the required input flow rate for power generation. Reducing the overall size of the separator can potentially decrease the supply flow rate. This approach mitigates concerns about bulk water transfer in and out of the reservoir affecting the salinity gradient and system stability. Furthermore, a lower flow rate could extend the lifespan of the cycle.

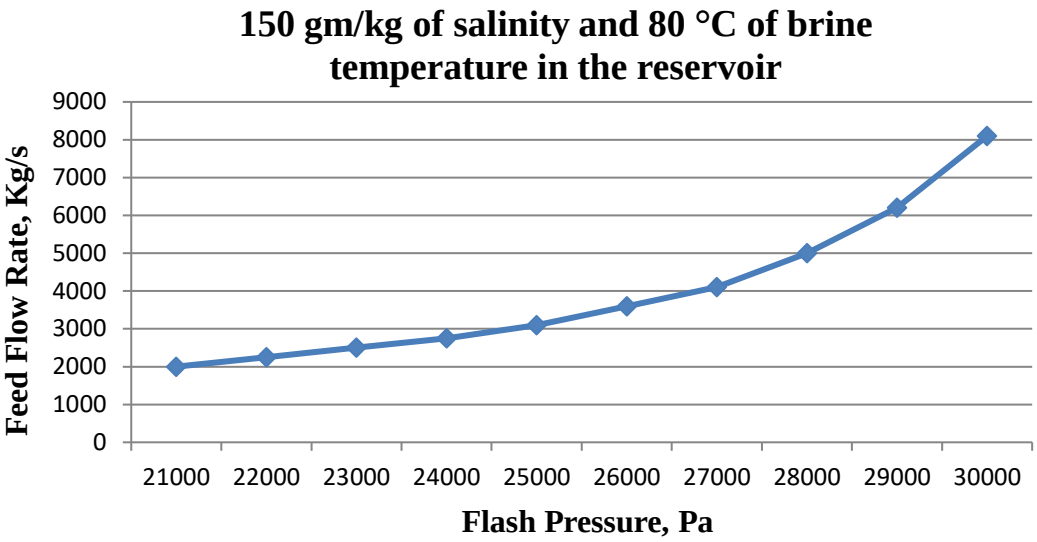

Fig. 12. Flash pressure variation in relation to feed flow rate

Increasing the reservoir's lower convection zone (LCZ) can potentially enhance the input heat to the separator, leading to a higher flash percentage of the hotter water, as illustrated in Figure 13.

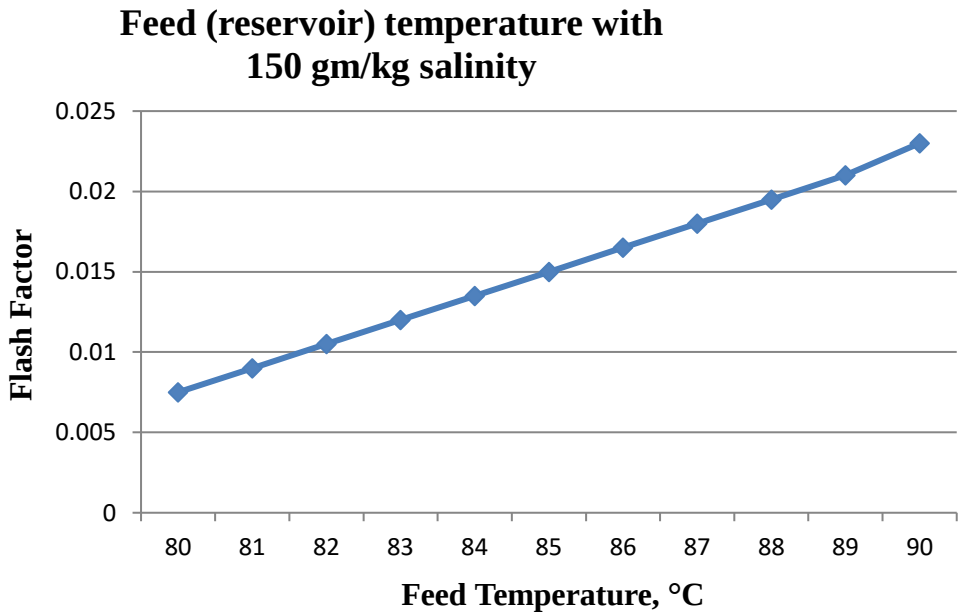

Fig. 13. Variation of feed temperature of brine vs. flash factor

As shown in Figure 14, water with a higher temperature could lead to a greater flash percentage. This, in turn, would decrease the required feed flow rate and reduce the overall size of the separator.

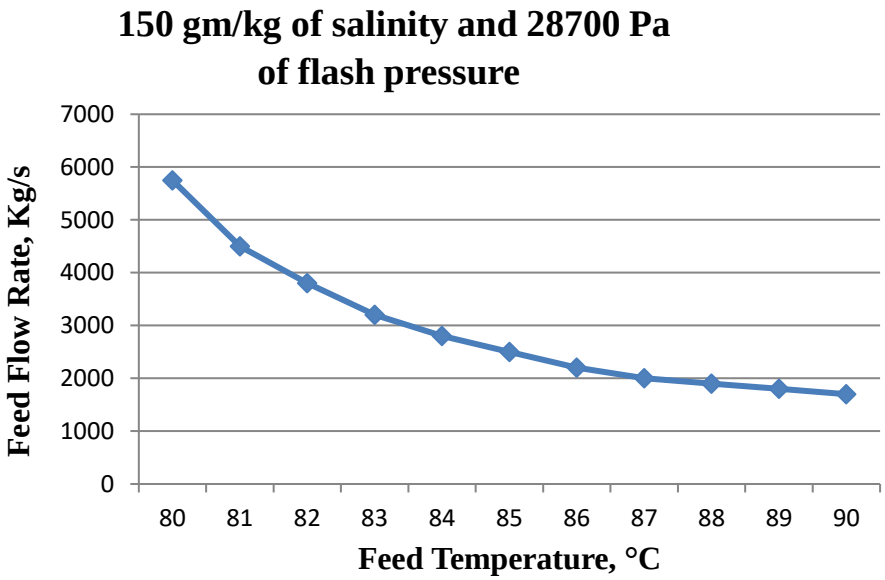

Fig. 14. Variation of feed temperature vs. FFR

Figure 15 depicts a positive correlation between system efficiency and feed temperature. This translates to a smaller reservoir requirement as fewer sunshine hours would be needed to generate the same amount of power.

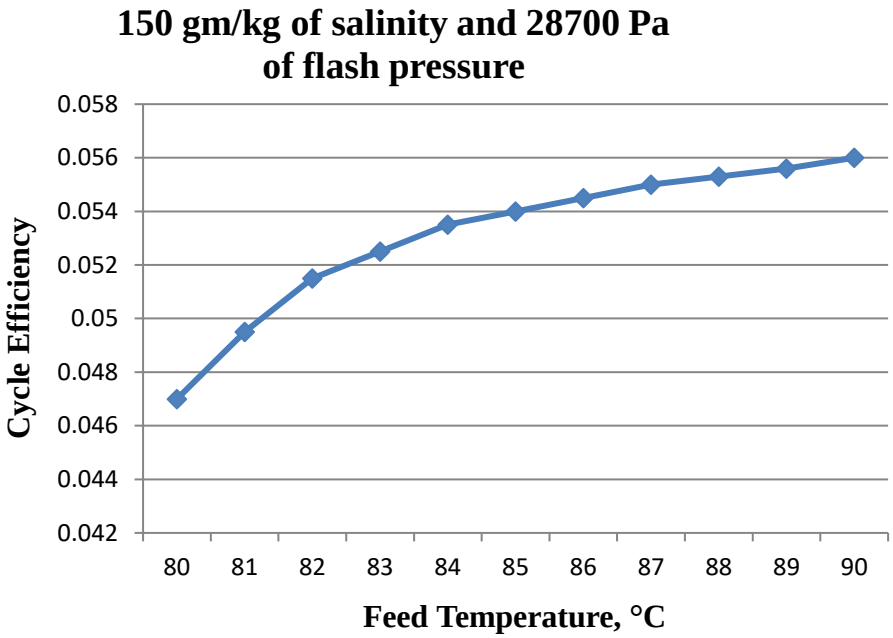

Fig. 15. Variation of feed temperature vs. cycle efficiency

Figure 16 to Figure 18 illustrate the variations in water properties (specific heat capacity, density, and dynamic viscosity) of the working fluid entering the flash separator throttle. These properties are determined by the temperature of the lower convection zone (LCZ), which acts as the heat source.

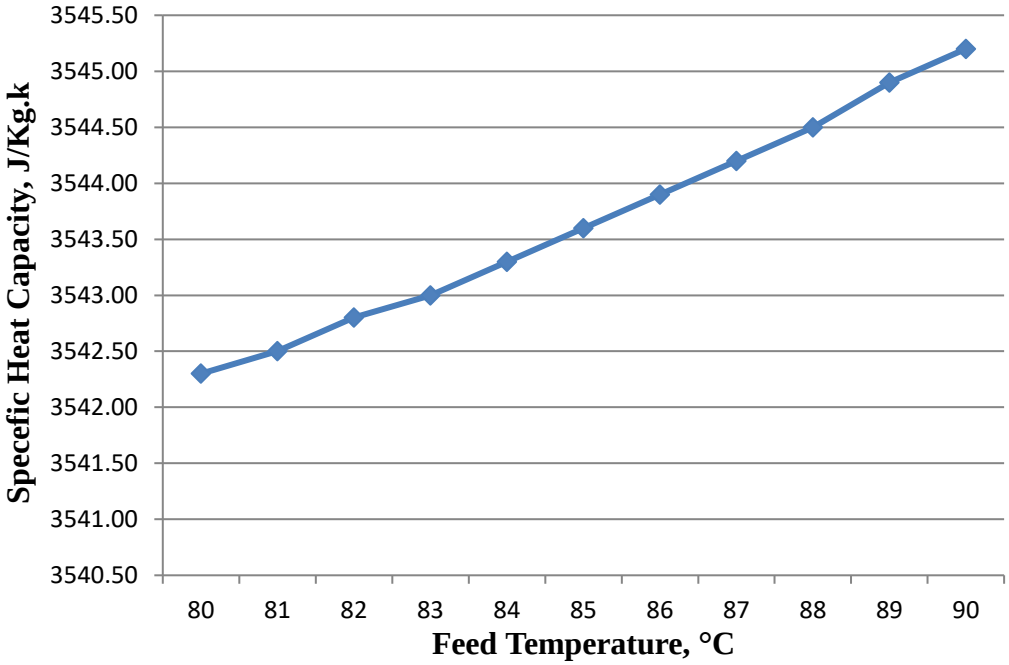

Fig. 16. Feed temperature vs. specific heat capacity of brine

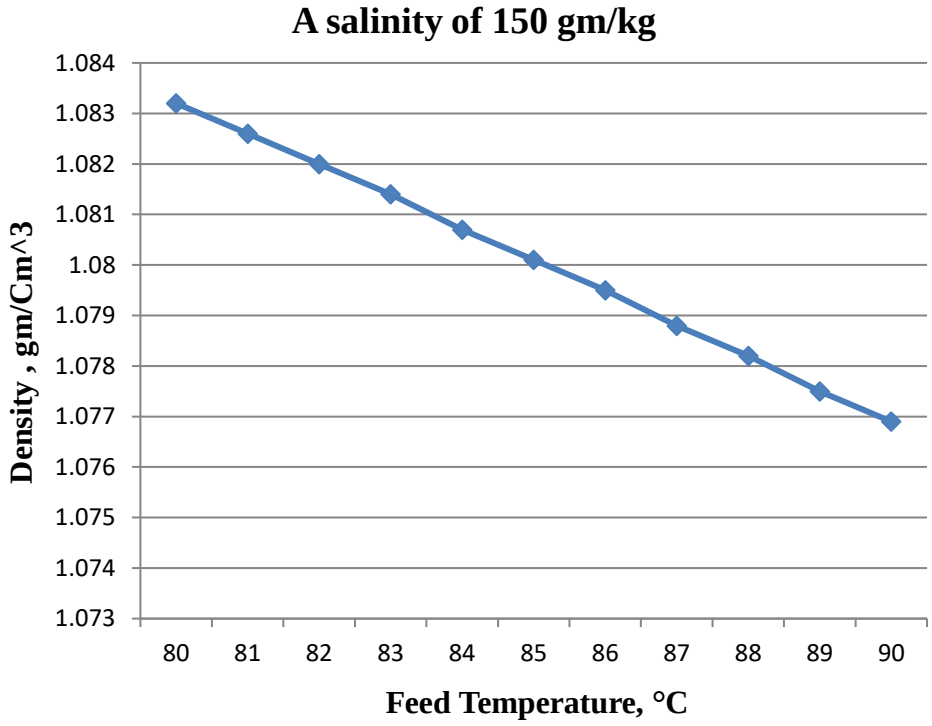

Fig. 17. Feed temperature vs. density

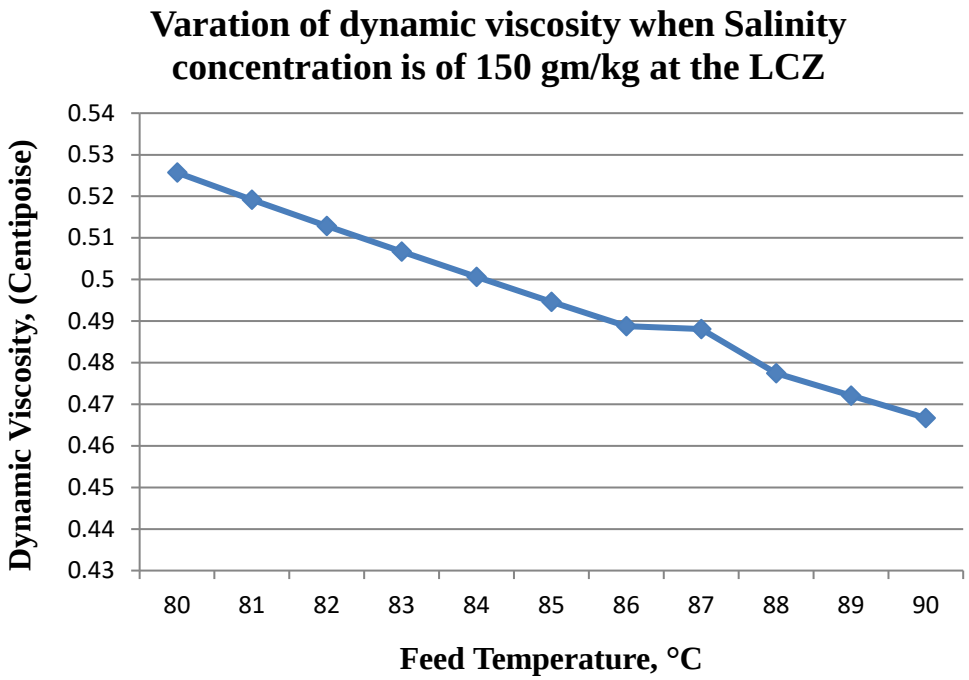

Fig. 18. Feed temperature vs. dynamic viscosity

5. Conclusion

The article presents a method for measuring solar radiation merely from geographical latitude. The accuracy of this technique is tested by comparing its forecasts to NASA's 22-year averaged data in three Middle Eastern locales, which show a high level of agreement. Both transient and steady-state models were investigated, however the steady-state model produced more accurate findings. The study also investigates the potential of solar reservoirs in cold areas, noting their capacity to achieve temperatures of 80°C with certain configurations. These reservoirs provide a feasible alternative to fossil fuel-based thermal energy in some industries, perhaps benefiting local economies dealing with unemployment. Potential uses include process refrigeration, desalination, heating, magnesium chloride synthesis, and improved salt yields. Given their potential, solar reservoirs might be a significant source of future energy.

While salinity gradient solar ponds (SGSPs) may not be much less expensive than other alternatives, they might be an attractive choice in areas with high power rates or restricted grid connection. Furthermore, taking into account additional factors such as avoiding waste disposal licences, the environmental advantages of using renewable energy, and potential tax breaks for using renewable sources, the real cost of SGSPs may be lower than previously thought. The study reported here recognises the limits of the explored design parameters. For example, the forecast of 80°C for LCZ heat was based exclusively on quantitative calculations. While the data point to promising efficiency for power production, the cycle might be improved by raising reservoir temperature (and input ambient temperature) or decreasing discharge pressure. These changes may optimise the flash separation process and improve overall cycle performance. The study also reveals difficulties with the flash cycle. The initial burst pressure necessary for plant operation would be relatively low, perhaps limiting the usage of a robust separator. Achieving the required flow rate for sufficient steam production at full turbine power was another difficulty. Overall, this study emphasises the promise of solar reservoirs as a renewable energy source, while also recognising existing limits and areas for additional investigation.

Acknowledgement
This research was not funded by any grant.

References
[1] Saxena, Abhishek, Erdem Cuce, Desh Bandhu Singh, Pinar Mert Cuce, Parul Gupta, Ajay Suryavanshi, Mahmoud Farrokhi, and A. A. El-Sebaii. "A thermodynamic review on solar ponds." *Solar Energy* 242 (2022): 335-363. https://doi.org/10.1016/j.solener.2022.07.016
[2] Vo, Thi Thu Em, Hyeyoung Ko, Jun-Ho Huh, and Namje Park. "Overview of solar energy for aquaculture: The potential and future trends." *Energies* 14, no. 21 (2021): 6923. https://doi.org/10.3390/en14216923
[3] Bacha, Habib Ben, A. S. Abdullah, and Mohamed Abdelgaied. "Design and development of a tubular solar distiller using a convex absorber, wick materials, and PCM reservoir combined with a solar parabolic concentrator." *Journal of Energy Storage* 62 (2023): 106897. https://doi.org/10.1016/j.est.2023.106897
[4] Verma, Vikas, Sivasakthivel Thangavel, Nitesh Dutt, Ashwani Kumar, and Rohitha Weerasinghe. "Introduction to thermal energy storage: Solar, geothermal and hydrogen energy." In *Highly Efficient Thermal Renewable Energy Systems*, pp. 1-22. CRC Press. https://doi.org/10.1201/9781003472629-1
[5] Ahmadizadeh, Mohammad, Milad Heidari, Sivasakthivel Thangavel, Eman Al Naamani, Morteza Khashehchi, Vikas Verma, and Ashwani Kumar. "Technological advancements in sustainable and renewable solar energy systems." In *Highly Efficient Thermal Renewable Energy Systems*, pp. 23-39. CRC Press, 2024. https://doi.org/10.1201/9781003472629-2
[6] Safi, M. J. "Performance of a flash desalination unit intended to be coupled to a solar pond." *Renewable Energy* 14, no. 1-4 (1998): 339-343. https://doi.org/10.1016/S0960-1481(98)00087-1
[7] Kundu, Arijit, Ashwani Kumar, Nitesh Dutt, Chandan Swaroop Meena, and Varun Pratap Singh. "Introduction to thermal energy resources and their smart applications." In *Thermal Energy Systems*, pp. 1-15. CRC Press, 2023. https://doi.org/10.1201/9781003395768-1
[8] Dewangan, Ashok K., Syed Quadir Moinuddin, Muralimohan Cheepu, Sanjeev K. Sajjan, and Ashwani Kumar. "Thermal energy storage: Opportunities, challenges and future scope." *Thermal Energy Systems* (2023): 17-28. https://doi.org/10.1201/9781003395768-2
[9] Al-Jabri, Hareb, Probir Das, Shoyeb Khan, Mahmoud Thaher, and Mohammed AbdulQuadir. "Treatment of wastewaters by microalgae and the potential applications of the produced biomass—a review." *Water* 13, no. 1 (2020): 27. https://doi.org/10.3390/w13010027
[10] Lu, Huanmin, John C. Walton, and Andrew HP Swift. "Desalination coupled with salinity-gradient solar ponds." *Desalination* 136, no. 1-3 (2001): 13-23. https://doi.org/10.1016/S0011-9164(01)00160-6
[11] Khashehchi, Morteza, Sivasakthivel Thangavel, Pooyan Rahmanivahid, Milad Heidari, Taleb Moazzeni, Vikas Verma, and Ashwani Kumar. "Solar desalination techniques: Challenges and opportunities." *Highly Efficient Thermal Renewable Energy Systems* (2024): 305-329. https://doi.org/10.1201/9781003472629-19
[12] Dogan, Mustafa Sahin, Josue Medellin-Azuara, and Jay R. Lund. "Hydropower Reservoir Optimization with Solar Generation-Changed Energy Prices in California." *Water Resources Management* 38, no. 6 (2024): 2135-2153. https://doi.org/10.1007/s11269-024-03747-6
[13] Al-Rubaye, Layth Abed Hasnawi, Lutfi Youssif Zaidan, and Ahmed Al-Samari. "Study the Investment Opportunity of Hybrid Energy Resources (Biomass and Solar) System; Iraq as a Case Study." *Journal of Advanced Research in Fluid Mechanics and Thermal Sciences* 105, no. 1 (2023): 107-121. https://doi.org/10.37934/arfmts.105.1.107121
[14] Danso, Derrick Kwadwo, Baptiste François, Benoit Hingray, and Arona Diedhiou. "Assessing hydropower flexibility for integrating solar and wind energy in West Africa using dynamic programming and sensitivity analysis. Illustration with the Akosombo reservoir, Ghana." *Journal of Cleaner Production* 287 (2021): 125559. https://doi.org/10.1016/j.jclepro.2020.125559
[15] Dah, M. M. Ould, M. Ouni, A. Guizani, and A. Belghith. "Study of temperature and salinity profiles development of solar pond in laboratory." *Desalination* 183, no. 1-3 (2005): 179-185. https://doi.org/10.1016/j.desal.2005.03.034
[16] Rabl, Ari, and Carl E. Nielsen. "Solar ponds for space heating." *Solar Energy* 17, no. 1 (1975): 1-12. https://doi.org/10.1016/0038-092X(75)90011-0
[17] Saleh, Ahmad. "Modeling and performance analysis of a solar pond integrated with an absorption cooling system." *Energies* 15, no. 22 (2022): 8327. https://doi.org/10.3390/en15228327
[18] Chitt, Mira, Sivasakthivel Thangavel, Vikas Verma, and Ashwani Kumar. "Green hydrogen productions: Methods, designs and smart applications." In *Highly Efficient Thermal Renewable Energy Systems*, pp. 261-276. CRC Press, 2024. https://doi.org/10.1201/9781003472629-16
[19] 19 Rana, S., A. Kumar, Y. Gori, and P. Patil. "Design and analysis of thermal contact conductance." *Journal of Critical Reviews* 6, no. 5 (2019): 363-370.

[20] Janusz-Szymańska, Katarzyna, Grzegorz Wiciak, Leszek Remiorz, and Dominik Hulak. "Heat Storage Using Solar Pond Technology and Post-Mining Brine-Preliminary Analysis." *Heat Transfer Engineering* (2024): 1-11. https://doi.org/10.1080/01457632.2024.2308353
[21] Abdulsalam, Alrowaished, Azni Idris, Thamer A. Mohamed, and Amimul Ahsan. "The development and applications of solar pond: a review." *Desalination and Water Treatment* 53, no. 9 (2015): 2437-2449. https://doi.org/10.1080/19443994.2013.870710
[22] El-Sebaii, Ahmed A., M. R. I. Ramadan, Saad Aboul-Enein, and A. M. Khallaf. "History of the solar ponds: a review study." *Renewable and Sustainable Energy Reviews* 15, no. 6 (2011): 3319-3325. https://doi.org/10.1016/j.rser.2011.04.008
[23] Kaushika, N. D. "Solar ponds: A review." *Energy Conversion and Management* 24, no. 4 (1984): 353-376. https://doi.org/10.1016/0196-8904(84)90016-5
[24] Emeara, Mohamed S., Ahmed Farouk AbdelGawad, and Emad Hamdy Ahmed. "Hybrid Renewable Energy System for a Sustainable House-Power-Supply." *Journal of Advanced Research in Fluid Mechanics and Thermal Sciences* 87, no. 1 (2021): 91-107. https://doi.org/10.37934/arfmts.87.1.91107
[25] Fauzi, Syafiqah Hanis Mohd, and Norazaliza Mohd Jamil. "Wastewater treatment process: A modified mathematical model for oxidation ponds." *Journal of Advanced Research in Fluid Mechanics and Thermal Sciences* 86, no. 1 (2021): 76-86. https://doi.org/10.37934/arfmts.86.1.7686
[26] Pant, Gunjan, Chandan Swaroop Meena, Anjali Saxena, Ashwani Kumar, Varun Pratap Singh, and Nitesh Dutt. "Study the temperature variation in alternate coils of insulated condenser cum storage tank: Experimental study." In *Biennial International Conference on Future Learning Aspects of Mechanical Engineering*, pp. 627-638. Singapore: Springer Nature Singapore, 2022. https://doi.org/10.1007/978-981-99-2382-3_52
[27] Gunerhan, Huseyin, and Arif Hepbasli. "Exergetic modeling and performance evaluation of solar water heating systems for building applications." *Energy and Buildings* 39, no. 5 (2007): 509-516. https://doi.org/10.1016/j.enbuild.2006.09.003
[28] 28Yadav, Jitendra, Varun Pratap Singh, and Ashwani Kumar. "Renewable energy technologies application in sustainable buildings." *Sustainable Technologies for Energy Efficient Buildings* (2024): 277. https://doi.org/10.1201/9781003496656-13
[29] 29Dutt, Nitesh, Ankush Hedau, Ashwani Kumar, Mukesh Kumar Awasthi, Sachin Hedau, and Chandan Swaroop Meena. "Thermo-hydraulic performance investigation of solar air heater duct having staggered D-shaped ribs: Numerical approach." *Heat Transfer* 53, no. 3 (2024): 1501-1531. https://doi.org/10.1002/htj.22998
[30] 30Torki, Zohir, Mohamed Benhamida, Zakaria Haddad, Azzedine Nahoui, Aissa Chouder, and Ibtissem Brahimi. "Effects of Temperature and Solar Radiation on Photovoltaic Modules Performances Installed in Oued Keberit Power Plant, Algeria." *Journal of Advanced Research in Fluid Mechanics and Thermal Sciences* 112, no. 1 (2023): 204-216. https://doi.org/10.37934/arfmts.112.1.204216
[31] 31Gasulla, Neus, Yusli Yaakob, Jimmy Leblanc, Aliakbar Akbarzadeh, and Jose Luis Cortina. "Brine clarity maintenance in salinity-gradient solar ponds." *Solar Energy* 85, no. 11 (2011): 2894-2902. https://doi.org/10.1016/j.solener.2011.08.028
[32] Valderrama, César, Oriol Gibert, Jordina Arcal, Pau Solano, Aliakbar Akbarzadeh, Enric Larrotcha, and José Luis Cortina. "Solar energy storage by salinity gradient solar pond: Pilot plant construction and gradient control." *Desalination* 279, no. 1-3 (2011): 445-450. https://doi.org/10.1016/j.desal.2011.06.035
[33] Wu, Xuan, Ting Gao, Chenhui Han, Jingsan Xu, Gary Owens, and Haolan Xu. "A photothermal reservoir for highly efficient solar steam generation without bulk water." *Science Bulletin* 64, no. 21 (2019): 1625-1633. https://doi.org/10.1016/j.scib.2019.08.022
[34] Kobayashi, Sachio, Hajime Imai, and Hisayoshi Yurimoto. "New extreme 16O-rich reservoir in the early solar system." *Geochemical Journal* 37, no. 6 (2003): 663-669. https://doi.org/10.2343/geochemj.37.663
[35] Sajid, Muhammad Usman, and Yusuf Bicer. "Comparative life cycle cost analysis of various solar energy-based integrated systems for self-sufficient greenhouses." *Sustainable Production and Consumption* 27 (2021): 141-156. https://doi.org/10.1016/j.spc.2020.10.025
[36] Karwa, Rajendra, and B. K. Maheshwari. "Heat transfer and friction in an asymmetrically heated rectangular duct with half and fully perforated baffles at different pitches." *International Communications in Heat and Mass Transfer* 36, no. 3 (2009): 264-268. https://doi.org/10.1016/j.icheatmasstransfer.2008.11.005
[37] Lei, Chengwang, and John C. Patterson. "Natural convection in a reservoir sidearm subject to solar radiation: a two-dimensional simulation." *Numerical Heat Transfer: Part A: Applications* 42, no. 1-2 (2002): 13-32. https://doi.org/10.1080/10407780290059404
[38] Leblanc, Jimmy, Aliakbar Akbarzadeh, John Andrews, Huanmin Lu, and Peter Golding. "Heat extraction methods from salinity-gradient solar ponds and introduction of a novel system of heat extraction for improved efficiency." *Solar Energy* 85, no. 12 (2011): 3103-3142. https://doi.org/10.1016/j.solener.2010.06.005

[39] Rubin, Hillel, and Giorgio A. Bemporad. "The advanced solar pond (ASP): basic theoretical aspects." *Solar Energy* 43, no. 1 (1989): 35-44. https://doi.org/10.1016/0038-092X(89)90098-4
[40] Tiwari, Anil Kr, and Aneesh Somwanshi. "Techno-economic analysis of mini solar distillation plants integrated with reservoir of garden fountain for hot and dry climate of Jodhpur (India)." *Solar Energy* 160 (2018): 216-224. https://doi.org/10.1016/j.solener.2017.11.078
[41] Tabrizi, Farshad Farshchi, and Ashkan Zolfaghari Sharak. "Experimental study of an integrated basin solar still with a sandy heat reservoir." *Desalination* 253, no. 1-3 (2010): 195-199. https://doi.org/10.1016/j.desal.2009.10.003
[42] Rghif, Yassmine, Daniele Colarossi, and Paolo Principi. "Salt gradient solar pond as a thermal energy storage system: A review from current gaps to future prospects." *Journal of Energy Storage* 61 (2023): 106776. https://doi.org/10.1016/j.est.2023.106776
[43] Rejab, Muhammad Nazri, Omar Mohd Faizan Marwah, Muhammad Akmal Johar, and Mohamed Najib Ribuan. "Real-time Thermal Energy Harvesting from Solar Radiation in Malaysia at Low-Temperature Difference." *Journal of Advanced Research in Fluid Mechanics and Thermal Sciences* 107, no. 2 (2023): 117-132. https://doi.org/10.37934/arfmts.107.2.117132